Solubilization of Docetaxel in Poly(ethylene oxide)-*block*-poly(butylene/styrene oxide) Micelles

Mahmoud Elsabahy,[†] Marie-Ève Perron,[†] Nicolas Bertrand,[†] Ga-er Yu,[‡] and Jean-Christophe Leroux*[,†,§]

Faculty of Pharmacy, University of Montreal, C.P. 6128, Succursale Centre-Ville, Montreal (QC) H3C 3J7, Canada, and Advanced Polymer Materials, Inc., 5020 Fairway, Suite 224, Montreal (QC) H8T 1B8, Canada

Received February 23, 2007; Revised Manuscript Received April 16, 2007

Poly(ethylene oxide)-*block*-poly(styrene oxide) (PEO-*b*-PSO) and PEO-*b*-poly(butylene oxide) (PEO-*b*-PBO) of different chain lengths were synthesized and characterized for their self-assembling properties in water by dynamic/static light scattering, spectrofluorimetry, and transmission electron microscopy. The resulting polymeric micelles were evaluated for their ability to solubilize and protect the anticancer drug docetaxel (DCTX) from degradation. The drug release kinetics as well as the cytotoxicity of the loaded micelles were assessed in vitro. All polymers formed micelles with a highly viscous core at low critical association concentrations (<10 mg/L). Micelle morphology depended on the nature of the hydrophobic block, with PBO- and PSO-based micelles yielding monodisperse spherical and cylindrical nanosized aggregates, respectively. The maximum solubilization capacity for DCTX ranged from 0.7 to 4.2% and was the highest for PSO micelles exhibiting the longest hydrophobic segment. Despite their high affinity for DCTX, PEO-*b*-PSO micelles were not able to efficiently protect DCTX against hydrolysis under accelerated stability testing conditions. Only PEO-*b*-PBO bearing 24 BO units afforded significant protection against degradation. In vitro, DCTX was released slower from the latter micelles, but all formulations possessed a similar cytotoxic effect against PC-3 prostate cancer cells. These data suggest that PEO-*b*-P(SO/BO) micelles could be used as alternatives to conventional surfactants for the solubilization of taxanes.

1. Introduction

Docetaxel (DCTX) is an anticancer drug that displays a broad spectrum of antitumor activity. It is currently approved for the treatment of advanced breast cancer, which remains a major cause of morbidity and mortality in women worldwide.[1,2] Furthermore, it has been used with success in patients with various tumors, including advanced non-small-cell lung cancer and ovarian cancer. Due to its poor aqueous solubility, DCTX is currently formulated in polysorbate 80 (Taxotere). This formulation is devoid of water because DCTX degrades over time in protic solvents.[2] The polysorbate 80 formulation is known to cause severe allergic reactions and peripheral neuropathy.[3,4] Early clinical studies of Taxotere revealed that the incidence of hypersensitivity reactions ranged from 5 to 40%.[4] Moreover, after dilution with the hydroalcoholic vehicle provided, the Taxotere formulation is physically unstable and must be administered to the patient within 8 h.

To overcome the disadvantages of the current formulation and to increase the therapeutic index of DCTX, various colloidal drug carriers, such as emulsions,[5] liposomes,[6] and nanoparticles,[7] are currently being investigated. Likewise, block copolymer micelles have recently attracted considerable attention for the delivery of taxanes.[8−12] In aqueous media, amphiphilic block copolymers can spontaneously self-assemble into nanoscopic core−shell-type structures having different morphologies (spheres, small rods, worm-like geometries, etc.),[13−16] wherein the hydrophobic blocks form the micelle core and the hydrophilic segments make up the corona. The hydrophobic core serves as a reservoir for poorly water-soluble drugs, while the hydrophilic shell interacts with the biological milieu and can alter the pharmacokinetics and biodistribution of the incorporated drug.[17]

Among the different amphiphilic block copolymers that have been evaluated for drug delivery applications, diblock copolymers of poly(ethylene oxide) (PEO) and poly(butylene oxide) (PBO) or poly(styrene oxide) (PSO) are of particular interest. These polymers can self-assemble at low concentrations into micelles of various shapes, depending on relative block lengths, concentration, and temperature.[18−21] Their hydrophobic segments exhibit low glass transition temperatures (ca. 40 °C), allowing for the incorporation of drugs at temperatures that are compatible with thermolabile agents.[22,23] Although PSO- and PBO-based copolymer micelles have been characterized in several studies,[18−21] their role as solubilizers has been reported only for the antifungal drug griseofulvin, which is of low clinical significance as it is currently administered orally in a micronized form.[22,24]

The aim of this project was to characterize the self-assembling properties of short PEO-*b*-PBOs and PEO-*b*-PSOs and assess their ability to dissolve and chemically protect DCTX. The molecular weight of the PEO segment was fixed at 2000, while the nature and length of the hydrophobic block were varied. The micelles were analyzed by light scattering, transmission electron microscopy (TEM), and fluorescence spectroscopy. The effect of micellar solubilization on the aqueous stability of DCTX was examined by high-performance liquid chromatography (HPLC). In addition, drug release and cytotoxicity were also evaluated in vitro.

* To whom correspondence should be addressed. Phone: (514) 343-6455. Fax: (514) 343-6871. E-mail: Jean-Christophe.Leroux@umontreal.ca.
[†] University of Montreal.
[‡] Advanced Polymer Materials, Inc.
[§] Canada Research Chair in Drug Delivery.

10.1021/bm070226v CCC: $37.00
Published on Web 06/19/2007

2. Materials

Methoxy-PEO and BO were purchased from Fluka via Sigma-Aldrich (Oakville, ON, Canada). Pyrene, SO, polysorbate 80, and 3-[4,5-dimethylthiaolyl]-2,5-diphenyl-tetrazolium bromide (MTT) were procured from Sigma-Aldrich. DCTX was kindly provided by the Shanghai Fudan Taxusal New Technology Co. (Shanghai, China). ^{14}C-labeled DCTX (60 mCi/mmol) was obtained from American Radiolabeled Chemicals, Inc. (St. Louis, MO). 1,3-bis-(1-pyrenyl)propane, RPMI medium, penicillin G, and streptomycin were obtained from Invitrogen Canada Co. (Burlington, ON, Canada). Two hundred-mesh copper grids, poly(L-lysine), and uranyl acetate for TEM sample preparation came from Canemco & Marivac, Inc. (Montreal, QC, Canada). Franz diffusion cells and membrane filters were purchased from Cole Parmer (Vernon Hills, IL) and Avestin (Ottawa, ON, Canada), respectively. PC-3 prostate cancer cells were purchased from American Type Culture Collection (Manassas, VA). Fetal bovine serum was purchased from Hyclone (Logan, UT). Ultima Gold was obtained from Perkin-Elmer (Woodbridge, ON, Canada). Deionized water was generated by a Millipore Milli-Q system (Bedford, MA).

3. Methods

3.1. Characterization of Unloaded Polymeric Micelles. *3.1.1. Synthesis and Characterization of Polymers.* $EO_{45}-SO_{26}$, $EO_{45}-SO_{15}$, $EO_{45}-BO_{24}$, and $EO_{45}-BO_{15}$ (subscripts denote number-average block lengths in repeat units) diblock copolymers were prepared by sequential oxyanionic polymerization, as described elsewhere.[25] Methoxy-PEO with a number-average molecular weight (M_n) of 2000 was partly converted to its potassium salt to initiate BO and SO polymerization. The monomers were dried over CaH_2 and were vacuum-transferred to ampoules containing activated PEO. The polymerization temperature was set at 80 °C. Weight-average molecular weight (M_w) and M_n were determined at 28 °C using a Waters gel permeation chromatography (GPC) system equipped with a 1515 isocratic pump and a 2410 refractive index detector (Waters, Milford, MA). Choloroform was the eluent, and monodisperse PEO was employed as standard. ^{1}H NMR spectra were recorded on a Bruker ARX400 spectrometer (Bruker, Milton, ON, Canada) in deuterated choloroform. The number of SO and BO units in each polymer was determined by ^{1}H NMR from eqs 1 and 2, respectively:

$$2(I_{4.2-5.0\text{ppm}}) + n\left(4 + \frac{3}{45}\right) = I_{3.2-3.9\text{ppm}} \quad (1)$$

$$3(I_{0.8-1.0\text{ppm}}) + n\left(4 + \frac{3}{45}\right) = I_{3.2-3.9\text{ppm}} \quad (2)$$

In both cases, n refers to the number of EO units, while the factor 3/45 takes into account the contribution of the methoxy end group of the PEO chain ($M_n = 2000$). In eq 1, $I_{4.2-5.0\text{ppm}}$ corresponds to the intensity of the methylene proton of the PSO backbone ($OCH_2CH(C_6H_5)$) and was set to 1. In turn, $I_{3.2-3.9\text{ppm}}$ corresponds to the intensity of the methylene groups of the PEO chain and methylene protons of the PSO backbone ($OCH_2CH(C_6H_5)$). Solving the equation for n allows the determination of an SO/EO ratio (where SO = 1) that can be balanced for PEO 2000 (45 EO units). Equation 2 is used in a similar fashion. In this case, $I_{0.8-1.0\text{ppm}}$ corresponds to the intensity of the methyl protons of the PBO pendant group ($OCH_2CH(CH_2CH_3)$) and was set to 3. On the other hand, $I_{3.2-3.9\text{ppm}}$ corresponds to the methylene groups of the PEO and PBO backbones.

3.1.2. Determination of the Critical Association Concentration (CAC). The apparent CAC of the polymers was estimated by a steady-state pyrene fluorescence method,[26] based on shifts of the third excitation band of pyrene from 333 to 336 and 339 nm due to its incorporation into the hydrophobic cores of PEO-*b*-PBO and PEO-*b*-PSO micelles, respectively. Serial dilutions of stock solutions of different copolymers were prepared to contain 2×10^{-7} M of pyrene and stirred overnight in the dark. Their excitation spectra were recorded at room temperature in an Aminco Bowman Series 2 luminescence spectrometer (Spectronic Instruments, Inc., Rochester, NY) at $\lambda_{em} = 390$ nm (bandpass = 2 nm). The CAC was determined from the intersection of two straight lines (the horizontal line with an almost constant value of the ratio $I_{336or339}/I_{333}$, and the vertical line with a steady increase in the ratio value) on the graph of the fluorescence intensity ratio $I_{336or339}/I_{333}$ versus log polymer concentration. Experiments were performed in triplicate.

3.1.3. Measurement of Core Viscosity. 1,3-Bis-(1-pyrenyl)-propane, a hydrophobic probe similar to pyrene, diffuses from an aqueous phase to the hydrophobic core of micelles. Given that the extent of excimer formation depends on the viscosity of the surrounding environment, the ratio of the excimer to monomer intensity (I_e/I_m) at 376 and 480 nm can be exploited to measure effective micelle core viscosity. 1,3-Bis-(1-pyrenyl)-propane was dissolved in 5 mL of chloroform to give a final concentration of 2×10^{-7} M. The solvent was then evaporated and replaced by 5 mL of aqueous polymer solutions at concentrations above the CAC (0.5 mg/mL). Sodium dodecyl sulfate (SDS) at 5 mg/mL served as a control, low molecular weight surfactant. The solutions were stirred for 24 h in the dark. The emission spectrum of 1,3-bis-(1-pyrenyl)propane was obtained at room temperature with an Aminco Bowman Series 2 luminescence spectrometer. The excitation wavelength and the emission bandwidth were set at 333 and 4 nm, respectively. All measurements were done in triplicate.

3.1.4. Dynamic Light Scattering (DLS) Measurements. The mean hydrodynamic diameters (d_h) and the polydispersity indices (PDIs) of polymeric micelles were measured by DLS with a Malvern Autosizer 4800 instrument (Malvern Instruments, Worcestershire, UK). All samples were filtered (Acrodisc 13-mm syringe filter with 0.45-μm nylon membrane, Pall Co., Mississauga, ON, Canada) prior to analysis. The different polymers were dissolved in water to a final concentration of 2 mg/mL. Measurements were taken at a fixed scattering angle of 90°. DLS measurements were also performed at different angles (50−140°) to examine micelle sphericity. For spherical particles, diameter is independent of detection angle due to the undetectable rotational motion.[27] The CONTIN program was used to extract size distributions from the autocorrelation functions. Measurements were performed in triplicate at room temperature.

3.1.5. Multiangle Static Light Scattering (MASLS) Measurements. Polymer solutions were prepared in Millipore water at room temperature and stirred overnight. All samples were passed through a 0.45-μm nylon filter prior to analysis. Then, samples were subjected to MASLS measurements in a Malvern Autosizer 4800 at six angles ranging from 50 to 120°, for five polymer concentrations above the CAC (0.25−2 mg/mL). The M_w values of the micelles were extracted from eq 3, which describes the intensity of light scattered from a dilute solution of macromolecules:

$$\frac{Kc}{R_0} = \frac{1}{M_w P(\theta)} + 2A_2c + 3A_3c^2 \quad (3)$$

In this equation, c stands for the polymer concentration, R_0 is the Rayleigh ratio of the solution, and A_2 and A_3 are the second and third virial coefficients. K is, in turn, defined by

$$K = \frac{4\pi^2 n_0^2 \left(\frac{dn}{dc}\right)^2}{\lambda^4 N} \quad (4)$$

where n_0 is the refractive index of the solvent, λ is the laser wavelength in vacuo, and N is Avogadro's number. Specific refractive index increments (dn/dc) were determined using a differential Rudolph J157 automatic refractometer (Rudolph Research Analytical, Flanders, NJ), at a wavelength of 589.3 nm. The dn/dc values for $EO_{45}-SO_{26}$, $EO_{45}-SO_{15}$, $EO_{45}-BO_{24}$, and $EO_{45}-BO_{15}$ solutions were 0.160, 0.154, 0.112, and 0.120 cm^3/g, respectively. Aggregation number (N_{agg}) was calculated by dividing the micelle M_w by that of the corresponding polymer. Radii of gyration (r_g) were also extracted from the MASLS analysis.

3.2. TEM. Copper grids (200 mesh) were coated with a drop of aqueous poly(L-lysine) solution (0.1% w/v) 5 min prior to sample deposition to ensure good adhesion between the samples and the grids. Excess solution was wicked off, the grids were allowed to dry, and a drop of different micelle solutions (2 mg/mL) was placed on the grid for 2 min. After the removal of excess solution, a droplet of uranyl acetate (3% w/v in water) was added to provide negative staining. After 5 min, the grids were gently washed with water, and excess fluid was removed with filter paper. The samples were then analyzed under a Philips CM100 transmission electron microscope (FEI Company, Tokyo, Japan) operating at 60 kV. Micrographs were taken at a magnification of 50 000.

3.3. Characterization of DCTX-Loaded Polymeric Micelles. *3.3.1. Preparation and Characterization of DCTX-Loaded Micelles.* Both DCTX and the polymer were dissolved in ethanol. The solvent was then evaporated under vacuum at room temperature and replaced by Millipore water, and the solutions were stirred overnight prior to analysis. The solutions of drug-loaded micelles were centrifuged (18 000*g*, 30 min), the supernatant was collected and passed through a 0.2-μm nylon filter. Drug concentration was assayed in the supernatant using a Waters HPLC system equipped with a 1525 binary pump, a 2487 dual wavelength absorbance detector, and Breeze chromatography software (Waters, Milford, MA). *N*-Heptylbenzamide served as the internal standard. The mobile phase consisted of acetonitrile, methanol, and water (48:11:41 v/v). The column was a Waters Nova-Pack C18, 60 Å 4 μm (3.9 × 300 mm). The flow rate, detection wavelength, temperature, and injection volume were set at 1 mL/min, 232 nm, 4 °C, and 55 μL, respectively. Size analyses were performed by DLS on freshly prepared micelles and freeze-dried formulations after reconstitution in water.

3.3.2. Determination of the Partition Coefficient (K_v). DCTX-loaded micelles were prepared with the drug present in large excess (2 mg) and increasing polymer concentrations (from 2 to 10 mg/mL). The solutions were stirred overnight and then centrifuged (18 000*g*, 30 min). Drug concentration was assayed in the supernatant with the HPLC method detailed above. K_v values were obtained by plotting the ratio of DCTX solubility in the presence of polymeric micelles (S_{tot}) over that in pure water ($S_w = 2$ μg/mL) against micellar concentration according to eq 5:[28]

$$S_{tot}/S_w = 1 + K_v \cdot C_{mic} \cdot V_m \quad (5)$$

where C_{mic} is the micellar concentration (defined as the polymer concentration minus the CAC divided by N_{agg}). V_m is given by

$$V_m = (M_{wmic} \cdot Q_h)/d_h \quad (6)$$

where V_m is the micellar partial molar volume, M_{wmic} is the micellar molecular weight (as determined by MASLS), and Q_h is the hydrophobic block weight fraction. The density of the core, d_h, was assumed to be that of a homopolymer of a hydrophobic segment of similar molecular weight.

3.4. Chemical Stability of DCTX-Loaded Micelles. DCTX-loaded micelles were subjected to accelerated stability testing by heating the polymer solutions at 50 °C for 24 h. The polymer concentrations (5 mg/mL) were kept above the CAC, and the drug concentration was set at 2 μg/mL in all solutions. At scheduled time intervals, samples were withdrawn and assayed by HPLC for intact DCTX, as described above. An aqueous solution of free DCTX was used as the control.

3.5. Calculation of Solubility Parameters by the Group Contribution Method. Total (δ_t) and partial (δ_d, δ_p, and δ_h) solubility parameters of the drug, PEO, PBO, and PSO blocks were calculated by the following four equations according to the group contribution method:

$$\delta_d = \frac{\sum F_{di}}{V} \quad (7)$$

$$\delta_p = \frac{\sqrt{\sum F_{pi}^2}}{V} \quad (8)$$

$$\delta_h = \sqrt{\frac{\sum E_{hi}}{V}} \quad (9)$$

$$\delta_t = \sqrt{\delta_d^2 + \delta_p^2 + \delta_h^2} \quad (10)$$

where F_{di}, F_{pi}, and E_{hi} describe the functional group contributions from van der Waals dispersion forces, dipole−dipole interactions, and hydrogen bonding, respectively.[29] The total molar volumes (V) of DCTX, PEO, PBO, and PSO polymer repeat units were obtained by the Fedors method.[30]

3.6. In Vitro Release Kinetics. DCTX-loaded polymeric micelles (0.7% (w/w) for $EO_{45}-BO_{24}$, 0.7 and 3.5% (w/w) for $EO_{45}-SO_{26}$), spiked with ^{14}C-labeled DCTX (2 μCi/mg DCTX) were prepared in phosphate buffered saline (PBS, pH 7.4) as previously described. The release of DCTX from the different formulations was studied by following the time course of drug transfer from the donor to the acceptor compartment using jacketed Franz diffusion cells. Both compartments were separated from each other by two superimposed 50-nm polycarbonate membranes. The release medium was maintained under continuous agitation (700 rpm) and at a constant temperature of 37 ± 0.2 °C using a circulating water bath. To ensure sink conditions, DCTX-loaded polymeric micelles were dispersed to a final drug concentration of 0.5 μg/mL in the donor compartment. At various time points, a 200-μL aliquot was withdrawn from the acceptor compartment and replaced by 200 μL of fresh PBS. Ultima Gold scintillation cocktail (5 mL) was added to the sample, and DCTX was quantified by radioactivity counting (Liquid Scintillation Analyzer, Tri-Carb 2100TR, Packard, Meridan, CT).

3.7. In Vitro Cytotoxicity Assay. PC-3 prostate cancer cells were maintained in RPMI 1640 supplemented with fetal bovine serum (10%) and penicillin G/ streptomycin (100 units/mL).

Table 1. Molecular Characteristics of PEO-*b*-PBO and PEO-*b*-PSO

copolymer [a]	M_n[a]	M_n[b]	M_w[b]	M_w/M_n[b]
$EO_{45}-BO_{15}$	3080	2700	2900	1.05
$EO_{45}-BO_{24}$	3730	3400	3600	1.05
$EO_{45}-SO_{15}$	3800	3000	3350	1.11
$EO_{45}-SO_{26}$	5120	3460	4150	1.20

[a] The subscripts denote the number of repeat units as measured by ^{1}H NMR. [b] Measured by GPC.

Table 2. Size, CAC, and Core Viscosity of Unloaded Micelles[a]

copolymer	d_h (nm)	PDI	CAC (mg/L) ± SD	I_e/I_m ± SD
$EO_{45}-BO_{15}$	16	0.04	9.5 ± 0.5	0.15 ± 0.01
$EO_{45}-BO_{24}$	21	0.07	4.0 ± 0.2	0.12 ± 0.02
$EO_{45}-SO_{15}$	19	0.06	4.5 ± 0.2	0.05 ± 0.01
$EO_{45}-SO_{26}$	21	0.17	1.5 ± 0.1	0.04 ± 0.01

[a] Mean of three independent experiments.

For the cytotoxicity assays, DCTX-loaded polymeric micelles (0.7% (w/w) for $EO_{45}-BO_{24}$, 0.7 and 3.5% (w/w) for $EO_{45}-SO_{26}$) were passed through 0.45-μm nylon filters, then the drug content was assayed by HPLC. DCTX-loaded micelles and the control DCTX solution mimicking Taxotere (polysorbate 80/ethanol/DCTX 72.8:24.3:2.9 wt%) were serially diluted in cell culture medium prior to their addition. Control unloaded micelles were tested at polymer/polysorbate 80 concentrations ranging from 7×10^{-7} to 4.2 mg/mL. Cells were seeded in 96-well plates at a density of 5×10^3 cells/well and cultured for 24 h at 37 °C in a humidified atmosphere containing 5% CO_2. The medium was then refreshed (100 μL) prior to the addition of 20-μL aliquots of either the micelle solutions or medium alone. After a 72-h incubation period, cells were rinsed with PBS, fed with 100 μL of fresh medium, and exposed to 10 μL/well of a MTT solution (5 mg/mL in PBS). After a 3.5-h incubation, 100 μL of an SDS solution (10% in HCl 0.01 N) was added to each well to dissolve the blue formazan product generated by the oxidation of MTT by living cells. The absorbance was read 16 h later at 570 nm using a Tecan Safire plate reader (Durham, NC).

4. Results and Discussion

4.1. Characterization of the Polymers and Unloaded Micelles. The molecular characteristics of PEO-*b*-PBO and PEO-*b*-PSO copolymers are reported in Table 1. Given that these polymers are not biodegradable, relatively low molecular weights were targeted (<6000) to avoid exceeding the renal filtration threshold for the elimination of unimers.[31,32] GPC revealed that PEO-*b*-PBOs had narrow distribution peaks, while the curves of PEO-*b*-PSOs showed a small shoulder on the low volume side of the main narrow peak, which was attributed to the initiation of homo-PSO by moisture (data not included). The PEO-*b*-PSOs were further purified by precipitation of the copolymers from a product solution of dichloromethane into hexane to give the final products with a single peak in GPC. ^{1}H NMR spectra were recorded and confirmed the compositions of the block copolymers.[33]

All polymers exhibited low CAC, ranging from 1 to 10 mg/L (Table 2). The CAC was found to decrease upon increasing hydrophobic chain length and substituting BO for SO. Indeed, the CAC of $EO_{45}-BO_{15}$ was twice that of the $EO_{45}-SO_{15}$ copolymer, reflecting the stronger hydrophobic interactions conferred by the aromatic ring. In a recent review, Booth et al.[34] ranked the relative hydrophobicities of various oxyalkylene units and attributed values of 1, 6, and 12 to propylene oxide, BO, and SO, respectively. All polymeric micelles possessed highly viscous cores, as evidenced by the low I_e/I_m ratios (0.05−0.12) compared to that of SDS (0.69), which is liquid-like (Figure 1 and Table 2). PSO-based micelles presented higher core viscosity than their PBO counterparts. The latter showed I_e/I_m values similar to those of PEO-*b*-poly(L-aspartamide) derivatives.[35]

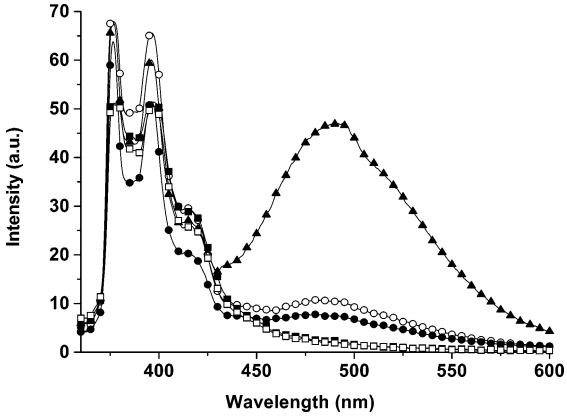

Figure 1. Fluorescence emission spectra of 1,3-bis-(1-pyrenyl)-propane in $EO_{45}-BO_{15}$ (○), $EO_{45}-BO_{24}$ (●), $EO_{45}-SO_{15}$ (□), $EO_{45}-SO_{26}$ (■), and SDS (▲) micellar aqueous solutions.

Table 3. MASLS Analysis of Unloaded Micelles

copolymer	M_{wmic}	N_{agg}	r_g/r_h[a]
$EO_{45}-BO_{15}$	263 500	90	0.9
$EO_{45}-BO_{24}$	1 193 700	330	0.9
$EO_{45}-SO_{15}$	1 030 700	307	1.3
$EO_{45}-SO_{26}$	1 235 000	310	3.6

[a] r_h is the hydrodynamic radius.

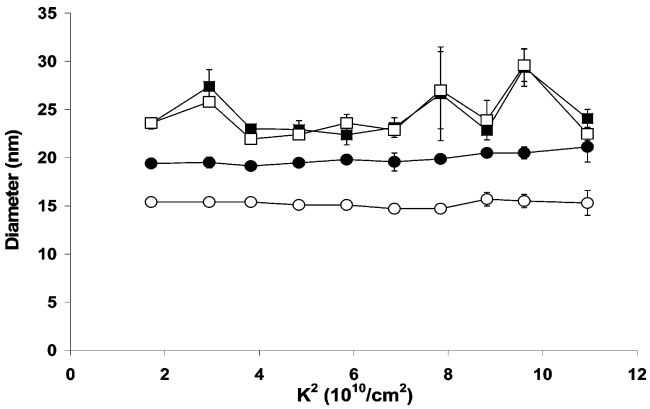

Figure 2. Change of diameter with the magnitude of K^2 for $EO_{45}-BO_{15}$ (○), $EO_{45}-BO_{24}$ (●), $EO_{45}-SO_{15}$ (□), and $EO_{45}-SO_{26}$ (■) micelles (detection angles 50−140°). Each value is the mean of three experiments ± SD. The mean diameter was found to be independent of the polymer concentration above the CAC.

The size of micelles is controlled by various factors, among which the length and nature of the core-forming segment and corona-forming chain are predominant. As reported in Table 2, the mean d_h of the micelles ranged from 16 to 21 nm. N_{agg} values were above 300 for all copolymers except $EO_{45}-BO_{15}$, which was about one-third of this value (Table 3). This polymer also formed the smallest micelles, as determined by DLS (16 nm). In all cases, size distribution was unimodal and of low polydispersity. Micelle diameter was augmented when the chain length of the oxyalkylene block was increased. The latter

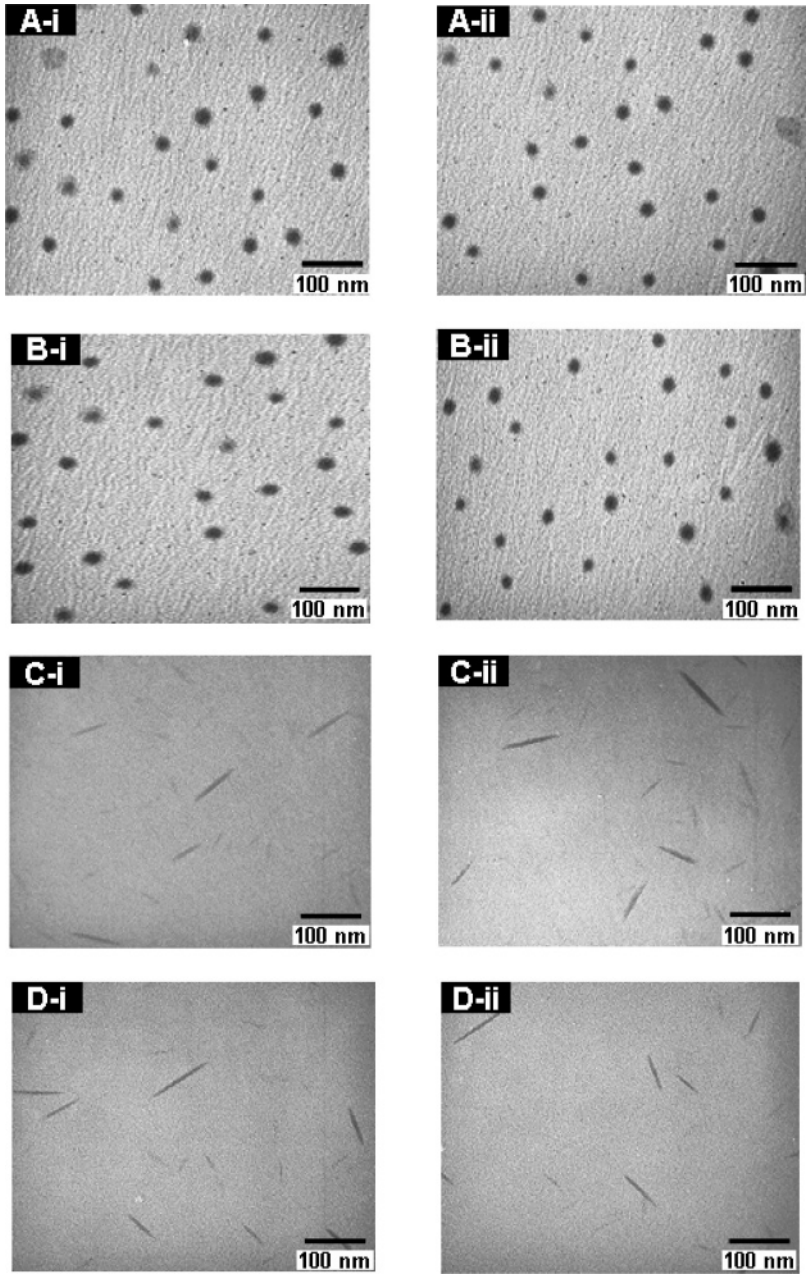

Figure 3. TEM imaging of unloaded (i) and DCTX-loaded (ii) $EO_{45}-BO_{15}$ (A), $EO_{45}-BO_{24}$ (B), $EO_{45}-SO_{15}$ (C), and $EO_{45}-SO_{26}$ (D) micelles.

observation is in agreement with earlier data obtained for similar systems.[19−21] DLS measurements were also performed at different angles (50−140°) to assess whether the micelles were spherical. Figure 2 shows the mean diameter as a function of the scattering vector (K^2). No angular dependence was found for $EO_{45}-BO_{24}$ and $EO_{45}-BO_{15}$ copolymers, the mean diameters being almost identical at every angle. This suggests that the BO polymers probably self-assembled into spheres. In contrast, angular dependence was evidenced in the case of both $EO_{45}-SO_{15}$ and $EO_{45}-SO_{26}$ copolymers, indicating that the self-assemblies were not spherical in shape.

The morphology of the unloaded micelles was then examined by computing the r_g/r_h ratio for the different polymers (Table 3). For PEO-*b*-PBO micelles, the r_g/r_h values were close to that of a hard sphere (0.78), in agreement with the formation of nearly spherical micelles. On the other hand, the ratios found for PEO-*b*-PSO copolymers were more than 1, consistent with significantly elongated micelles.[36] TEM imaging was undertaken in order to directly visualize the shape of the aggregates. As anticipated, PEO-*b*-PBO formed nearly spherical micelles in water (Figure 3, panels A-i and B-i), whereas the PEO-*b*-PSOs self-assembled into small rods (Figure 3, panels C-i and D-i). Under TEM, the diameters of all micelles were close to those obtained by DLS, while the mean length of the $EO_{45}-SO_{15}$ and $EO_{45}-SO_{26}$ rods were approximately 80 ± 15 and 90 ± 10 nm ($n = 20$), respectively. PSO-based micelles have been proposed to adopt both spherical and cylindrical arrangements, depending on the length of the respective PSO and PEO blocks. Indeed, Crothers et al.[37] found that the r_g/r_h of EO_{45}-*b*-SO_{10} micelles (same PEO length but shorter PSO block) was consistent with spherical micelle formation, thus confirming the determining role of polymer hydrophilic/ hydrophobic balance on micelle morphology.[38] In another study, Yang et al.[21] compared the N_{agg} of $EO_{17}-BO_8$ and $EO_{17}-SO_8$. These polymers have lower molecular weight than that of those studied in the present work, but their EO/BO and EO/SO ratios are comparable. They found that substituting BO for SO brought about a rise of N_{agg}, which was superior to the theoretical

Table 4. Characteristics of DCTX-Loaded Micelles

copolymer	$S_{CP} \pm$ SD (mg/g)[a]	Q_h	ρ (g/cm^3)[b]	$K_v \times 10^{-4}$	d_h (nm)	PDI
$EO_{45}-BO_{15}$	4.2 ± 0.8	0.35	0.973	3.9	17	0.07
$EO_{45}-BO_{24}$	7.4 ± 1.1	0.46	0.973	5.3	22	0.08
$EO_{45}-SO_{15}$	34.8 ± 1.7	0.47	1.150	35.3	19	0.07
$EO_{45}-SO_{26}$	41.7 ± 1.2	0.60	1.150	36.7	21	0.19

[a] Solubilizing capacity expressed as milligrams of DCTX per gram of copolymer. [b] The densities of the hydrophobic block were taken from the literature.[21,24]

increase expected for spherical micelles. They hypothesized that the difference in N_{agg} between these two polymers could be explained by elongation of the micelles to accommodate the high N_{agg}. While the formation of rod micelles with PEO-*b*-PSO has been predicted theoretically,[21,22] this is the first time that the cylindrical morphology of PSO-based micelles has been observed. Although the difference in shape between the two types of micelles can be related to differences in the hydrophobicity (being twice for the SO)[34] and conformations of BO and SO, it is worth mentioning that the possible residual homopolymer of SO dissolved in the micelle core may also have contributed to the formation of cylindrical PEO-*b*-PSO micelles.[39]

4.2. Characterization of DCTX-Loaded Micelles. The drug-loaded micelles were prepared according to a procedure that was initially proposed for PEO-*b*-poly(D,L-lactide) (PEO-*b*-PDLLA).[40] Attempts at dissolving DCTX into preformed micelles resulted in low drug loading, probably because of slow diffusion of the drug into the viscous micelle core (data not shown). Accordingly, it was decided to first codissolve both the drug and polymer in a pharmaceutically acceptable organic solvent (i.e., ethanol) to form a homogeneous polymeric matrix, evaporate the organic solvent, and then add the water phase. The size of the DCTX-loaded micelles was measured by DLS (Table 4), and no difference was observed compared to unloaded micelles. Moreover, the loaded micelles preserved their initial shape (Figure 3, panels A-ii−D-ii). The micelles could be readily freeze-dried, and recovered their initial size distribution upon reconstitution in aqueous media (data not shown). In solution, no crystallization was apparent for at least 14 days. The solubilizing capacity (S_{CP}) of each system was evaluated (Table 4). PSO-based micelles incorporated more DCTX (~3−4%) than did PBO micelles (<1%), most likely because of the better compatibility between DCTX and PSO (see below) and the micelle morphology. Micelles of cylindrical shape are usually associated with greater S_{CP}, given their higher N_{agg} and core volume.[22,24] Indeed, Crothers et al.[22] demonstrated that griseofulvin was also incorporated to a greater extent into PSO versus PBO micelles having comparable characteristics. For both polymers, S_{CP} rose when the length of the hydrophobic block was increased. More than 4% (w/w) drug loading could be achieved with $EO_{45}-SO_{26}$. With such loading, hydrosolubility exceeding 2 mg/mL was reached, which was more than 1000 times the aqueous solubility of free DCTX.

The K_v of DCTX between water and the copolymer micelles was calculated using eqs 5 and 6 (Table 4). The K_v values ranged from 4×10^4 to 53×10^4. The high affinity of DCTX for another hydrophobic block, that is, PDLLA, was reported previously by our group.[41] The K_v value of DCTX in poly(*N*-vinyl-2-pyrrolidone)-*block*-PDLLA micelles was found to be 2.46×10^4. It is similar to the K_v of the drug in PEO-*b*-PBO micelles, but substantially lower than the K_v for PEO-*b*-PSO.

Table 5. Total (δ_t) and Partial (δ_d, δ_p, and δ_h) Solubility Parameters of DCTX and Individual Polymer Blocks (MPa$^{1/2}$)

molecule	δ_d	δ_p	δ_h	δ_t
DCTX	20.6	3.1	14.6	25.5
PEO	17.8	11.1	9.1	22.9
PBO	16.6	5.8	6.6	18.8
PSO	20.8	4.6	5.8	22.1

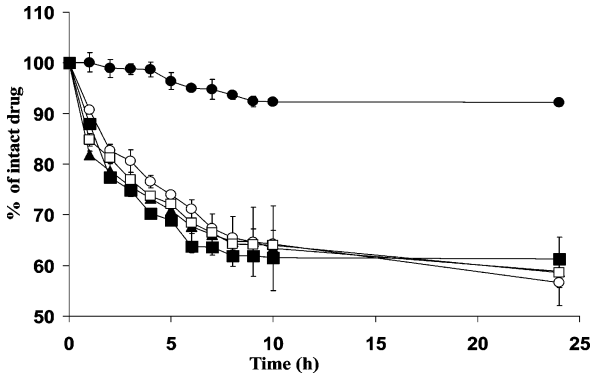

Figure 4. Effect of micellar solubilization on DCTX stability in $EO_{45}-BO_{15}$ (○), $EO_{45}-BO_{24}$ (○), $EO_{45}-SO_{15}$ (□), and $EO_{45}-SO_{26}$ (■) micelles. The stability of free DCTX in water (▲) is also shown. The experiments were carried out at a fixed temperature (50 °C) for 24 h. DCTX loading and concentration were set at 0.04 (% w/w) and 2 μg/mL, respectively. Mean ± SD ($n = 3$).

Solubility parameters are useful to estimate compatibility, interactions, and miscibility between drugs and various carrier systems.[41] The difference in loading capacity and the affinity of PEO-*b*-PSO and PEO-*b*-PBO for the drug were correlated with the solubility parameters and the enthalpy of mixing of both the drug and the polymers. As expected, the difference between the total solubility parameters of DCTX and each polymer block was found to be least important for PSO (Table 5). The enthalpy of mixing (ΔH_M) was then calculated using eq 11:[42]

$$\Delta H_M = \phi_1\phi_2[(\delta_{d1} - \delta_{d2})^2 + (\delta_{p1} - \delta_{p2})^2 + (\delta_{h1} - \delta_{h2})^2] \quad (11)$$

where ϕ_1 and ϕ_2 are volume fractions of the drug and the polymers. The ΔH_M values for PSO and PBO were 79.7 and 87.3 MPa, respectively, corroborating the experimental data. Considering the differences in both the solubility parameters and ΔH_M, PSO is more suitable than PBO for solubilizing DCTX.

4.3. In Vitro Evaluation of Micelle Formulations. The effect of micellar solubilization on the chemical stability of DCTX in water was investigated over a period of 24 h at 50 °C (Figure 4). For comparison between the different systems, all micelles were loaded at the same drug level (0.04% w/w). Despite their higher affinity for the drug, both PSO-based micelles were inefficient at protecting DCTX from degradation under accelerated stability testing conditions. Likewise, $EO_{45}-BO_{15}$ did not afford any protection compared to the control drug solution. Surprisingly, only $EO_{45}-BO_{24}$ was able to preserve most of the DCTX chemical integrity (92%) after 24 h. This protective effect cannot be accounted for by differences between the drug affinity or core microviscosity of the BO_{24} block, since both parameters were inferior to those of the PSO block and almost similar to the BO_{15} segment (Tables 2, 4, and 5). One possible explanation for the observed effect is the difference in specific surface area between the micelles. The specific surface

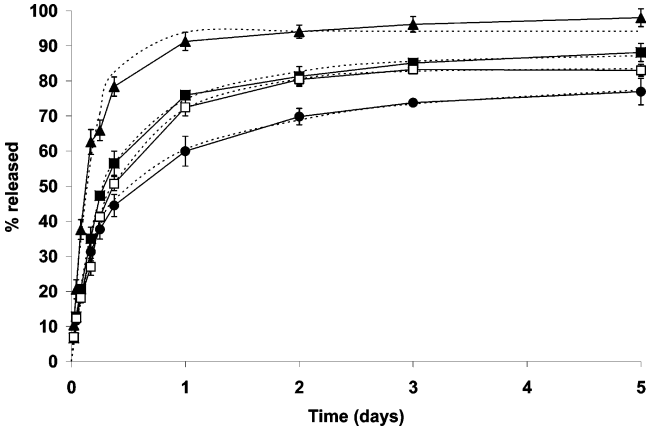

Figure 5. In vitro release kinetics of DCTX from $EO_{45}-BO_{24}$ (0.7% DCTX) (●), $EO_{45}-SO_{26}$ (0.7% DCTX) (□), and $EO_{45}-SO_{26}$ (3.5% DCTX) (■) micelles. DCTX diffusion in the absence of micelles is represented by (▲). The experiments were carried out at 37 °C in PBS (pH 7.4). Mean ± SD ($n = 3$). The dotted lines represent the simulated release kinetics.

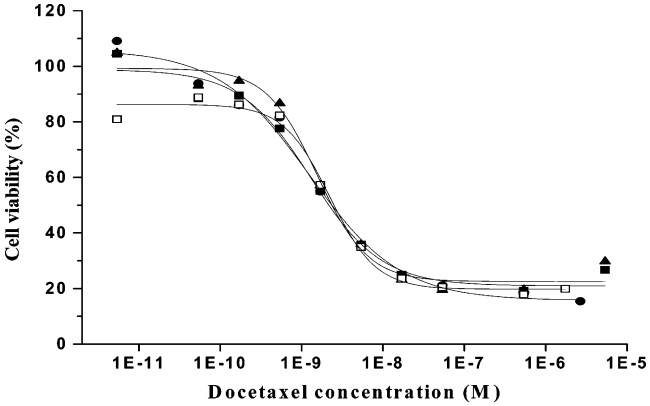

Figure 6. Cell viability of PC-3 cells exposed to $EO_{45}-BO_{24}$ (0.7% DCTX) (●), and $EO_{45}-SO_{26}$ (□) (0.7% DCTX), and (3.5% DCTX) EO_{45}-SO_{26} (■) DCTX-loaded micelles. A polysorbate 80/ethanol formulation of DCTX was used as control (▲). The data represent the mean of three experiments. For the purpose of clarity, the error bars of the standard deviation are omitted (coefficient of variation < 12%).

area (S) was estimated for spherical and cylindrical micelles using eqs 12 and 13, respectively:

$$S = 4\pi r^2/M_w \tag{12}$$

$$S = 2\pi rL/M_w \tag{13}$$

where L is the length of the cylindrical micelles, which was extracted from TEM analysis, r is the micelle radius (Table 4), and M_w is the molecular weight of micelles as ascertained by MASLS. BO_{24} micelles yielded the lowest specific surface area (760 m^2/g), whereas the calculated values for BO_{15}, SO_{15}, and SO_{26} micelles were 2050, 2800, and 2900 m^2/g, respectively. Thus, the greater protection conferred by $EO_{45}-BO_{24}$ micelles could be partially ascribed to decreased interactions of DCTX with the aqueous medium at the water−micelle interface due to the lower specific surface area.

The release of DCTX from $EO_{45}-BO_{24}$ and $EO_{45}-SO_{26}$ micelles was studied in vitro (Figure 5). The free drug diffused completely in about 24 h, indicating that the two superimposed 50-nm membranes influenced the release rate. However, this particular setting was necessary to prevent the transfer of micelles in the acceptor compartment (<5% after 5 days as estimated by DLS). All micelle formulations displayed similar profiles characterized by a fast initial release (~50% within 12 h) followed by a decelerated rate over 5 days. In order to eliminate the background effect, mathematical kinetic modeling was performed. In the model, the drug release measured in the acceptor compartment was divided into two different transfer rates, namely, one from micelles to the donor compartment and one from the donor to the acceptor compartment. Each transfer relation was defined by a simple first-order linear differential equation defined by microconstant K_m for the rate of DCTX release from micelles and K_d for the transfer of DCTX to the acceptor compartment (see Supporting Information). To assess the effect of the two superimposed 50-nm membranes on the release, K_d was determined by fitting the equation on the free DCTX release curve and was subsequently used to obtain the specific K_m of each formulation. Comparison of the release rates of the formulations with 0.7% DCTX showed that release was faster for $EO_{45}-SO_{26}$ than for $EO_{45}-BO_{24}$ micelles ($K_{mSO26} = 1.31\ d^{-1}$ vs $K_{mBO24} = 0.57\ d^{-1}$, and 83% of the drug had diffused out in 72 h vs 73%, respectively). However, normalization of the constants by specific surface area ($K_{mSO26}/S = 4.51\ 10^{-4}\ g\cdot m^{-2}\cdot d^{-1}$ vs $K_{mBO24}/S = 7.56\ 10^{-4}\ g\cdot m^{-2}\cdot d^{-1}$) tends to ascribe this difference to the surface dissimilarities between formulations, as previously discussed. Comparison of the release profiles of $EO_{45}-SO_{26}$ formulations with different drug loadings (0.7 and 3.5% DCTX) revealed that surface area was not the only factor affecting drug release. Indeed, similar release profiles were obtained despite the fact that there was a 5-fold difference in micelle concentrations between the two formulations. The drug loading may influence DCTX distribution in the micelles or its initial partition between micelles and the donor compartment and therefore affect the drug release profile.

The antimitotic activity of DCTX-loaded micelles was then evaluated on human prostate cancer cells PC-3. The cytotoxicity assays revealed that $EO_{45}-BO_{24}$ and $EO_{45}-SO_{26}$ micelle formulations were as efficient as the control commercial formulation to inhibit the growth of these cells (Figure 6). No difference was found between the tested systems with IC_{50} values ranging from 2.2 to 2.5 nM (±0.3 nM). Indeed, the in vitro release data can be used to rationalize these results. After 72 h of incubation, most of the DCTX had been released from the polymeric micelles and was thus available to exert its cytotoxic activity. Indeed, Le Garrec et al.[8] obtained similar findings with biodegradable poly(*N*-vinylpyrrolidone)-*b*-PDLLA micelles loaded with DCTX. These micelles exhibited IC_{50} values comparable to those of Taxotere, indicating the complete release of drug from the hydrophobic core. Neither the unloaded-micelles nor polysorbate 80 caused a significant decrease in cell viability up to a polymer/polysorbate 80 concentration of 0.01 mg/mL (corresponding to a DCTX concentration of 5.4×10^{-9} M for the micelles loaded with 0.7% drug) (data not shown). At high concentration (0.7 mg/mL), $EO_{45}-SO_{26}$ was fairly less toxic (86% viability) than polysorbate 80 (51% viability) and $EO_{45}-BO_{24}$ (24% viability). Altogether, these data suggest that, at high drug concentrations, PEO-*b*-PSO may potentially improve the therapeutic index of DCTX by decreasing the formulation's nonspecific toxicity.

5. Conclusion

In water, PEO-*b*-PBO and PEO-*b*-PSO block copolymers self-assembled at low concentrations to form spherical and cylindrical micelles, respectively. These micelles possessed diameters ranging from 16 to 21 nm, which make them suitable for sterilization by filtration and administration by intravenous

injection. PSO-based copolymers were associated with higher solubilizing capacities for DCTX (~4% w/w) than PBO due to the aromatic structure of the core-forming polymer and the cylindrical morphology of the resulting micelles. However, the PBO copolymer offered a greater protective effect against the hydrolytic degradation of DCTX. Nevertheless, the long-term stability for all these systems is guaranteed by the fact that the micelles investigated in this work could be lyophilized and thus stored in dried form. Such polymers could provide useful alternatives to low molecular weight surfactants for the solubilization of taxane derivatives.

Acknowledgment. This work was supported financially by the Canada Research Chair Program. Geneviève Gaucher and Marie-Hélène Dufresne are acknowledged for their critical reading of the manuscript.

Supporting Information Available. Equation and schematic illustration for the kinetic model proposed for DCTX release from micelles in jacketed Franz diffusion cells. This material is available free of charge via the Internet at http://pubs.acs.org.

References and Notes

(1) Walker, R. A.; Jones, J. L.; Chappell, S.; Walsh, T.; Shaw, J. A. *Cancer Metastasis Rev.* **1997**, *16*, 5.
(2) Rao, B. M.; Chakraborty, A.; Srinivasu, M. K.; Devi, M. L.; Kumar, P. R.; Chandrasekhar, K. B.; Srinivasan, A. K.; Prasad, A. S.; Ramanatham, J. *J. Pharm. Biomed. Anal.* **2006**, *41*, 676.
(3) Ardavanis, A.; Tryfonopoulos, D.; Yiotis, I.; Gerasimidis, G.; Baziotis, N.; Rigatos, G. *Anti-Cancer Drugs* **2004**, *15*, 581.
(4) Tije, A. J.; Verweij, J.; Loos, W. J.; Sparreboom, A. *Clin. Pharmacokinet.* **2003**, *42*, 665.
(5) Einhaus, C. M.; Retzinger, A. C.; Perrotta, A. O.; Dentler, M. D.; Jakate, A. S.; Desai, P. B.; Retzinger, G. S. *Clin. Cancer Res.* **2004**, *10*, 7001.
(6) Immordino, M. L.; Brusa, P.; Arpicco, S.; Stella, B.; Dosio, F.; Cattel, L. *J. Control. Release* **2003**, *91*, 417.
(7) Farokhzad, O. C.; Cheng, J.; Teply, B. A.; Sherifi, I.; Jon, S.; Kantoff, P. W.; Richie, J. P.; Langer, R. *Proc. Natl. Acad. Sci. U.S.A.* **2006**, 103, 6315.
(8) Le Garrec, D.; Gori, S.; Karkan, D.; Luo, L.; Lessard, D. G.; Smith, D.; Ranger, M.; Yessine, M. A.; Leroux, J. C. *J. Drug Deliv. Sci. Technol.* **2005**, *15*, 115.
(9) Kataoka, K.; Harada, A.; Nagasaki, Y. *Adv. Drug Deliv. Rev.* **2001**, *47*, 113.
(10) Kim, S. C.; Kim, D. W.; Shim Y. H.; Bang J. S.; Oh, H. S.; Kim, S. W.; Seo, M. H. *J. Control. Release* **2001**, *72*, 191.
(11) Jeong, Y. I.; Kang, M. K.; Sun, H. S.; Kang, S. S.; Kim, H. W.; Moon, K. S.; Lee, K. J.; Kim, S. H.; Jung, S. *Int. J. Pharm.* **2004**, *273*, 95.
(12) Kang, N.; Perron, M.; Prud'homme, R. E.; Zhang, Y.; Gaucher, G.; Leroux, J.-C. *Nano Lett.* **2005**, *5*, 315.
(13) Fairclough, J. P. A.; Norman, A. I.; Shaw B.; Nace, V. M.; Heenan, R. K. *Polym. Int.* **2006**, *55*, 793.
(14) Liu, L.; Gao, X.; Cong, Y.; Li, B.; Han, Y. *Macromol. Rapid Commun.* **2006**, *27*, 260.
(15) Castelletto, V.; Hamley, I. W. *Adv. Polym. Technol.* **2006**, *17*, 137.
(16) Norman, A. I.; Ho, D. L.; Lee, J. H.; Karim, A. *J. Phys. Chem. B* **2006**, *110*, 62.
(17) Hamaguchi, T.; Matsumura, Y.; Suzuki, M.; Shimizu, K.; Goda, R.; Nakamura, I.; Nakatomi, I.; Yokoyama, M.; Kataoka, K.; Kakizoe, T. *Br. J. Cancer* **2005**, *92*, 1240.
(18) Hamley, I. W.; Pedersen, J. S.; Booth, C.; Nace, V. M. *Langmuir* **2001**, *17*, 6386.
(19) Kelarakis, A.; Mai, S. M.; Havredaki, V.; Nace, V. M.; Booth, C. *Phys. Chem. Chem. Phys.* **2001**, *3*, 4037.
(20) Kelarakis, A.; Havredaki, V.; Booth, C.; Nace, V. M. *Macromolecules* **2002**, *35*, 5591.
(21) Yang, Z.; Crothers, M.; Attwood, D.; Collett, J. H.; Ricardo, N. M. P. S.; Martini, L. G. A.; Booth, C. *J. Colloid Interface Sci.* **2003**, *263*, 312.
(22) Crothers, M.; Zhou, Z.; Ricardo, N. M. P. S.; Yang, Z.; Taboada, Z.; Chaibundit, C.; Attwood, *D.;* Booth, C. *Int. J. Pharm*. **2005**, 293, 91.
(23) Zhou, Z.; Lodge, T. P.; Bates, F. S. *J. Phys. Chem. B* **2006**, *110*, 3979.
(24) Chaibundit, C.; Ricardo, N. M. P. S.; Crothers, M.; Booth, C. *Langmuir* **2002**, *18*, 4277.
(25) Mai, S.-M.; Ludhera, S.; Heatley, F.; Attwood, D.; Booth, C. *J. Chem. Soc., Faraday Trans.* **1998**, *94*, 567.
(26) Wilhelm, M.; Zhao, C. L.; Wang, Y.; Xu, R.; Winnik, M. A.; Mura, J. L.; Riess, G.; Croucher, M. D. *Macromolecules* **1991**, *24*, 1033.
(27) Yasugi, K.; Nagasaki, Y.; Kato, M.; Kataoka, K. *J. Control. Release* **1999**, *62*, 89.
(28) Krishna, A. K.; Flanagan, D. R. *J. Pharm. Sci.* **1989**, *78*, 574.
(29) Krevelen, D. V. Cohesive properties and solubility. In Krevelen, D. V., editor properties of polymers: their correlation with chemical structure; their numerical estimation and prediction from addition group contributions, 3rd ed., New York: Elsevier Scientific Publishing Co., 1990, p 189.
(30) Fedors, R. F. *Polym. Eng. Sci.* **1974**, *14*, 147.
(31) Yamamoto, Y.; Nagasaki, Y.; Kato, Y.; Sugiyama, Y.; Kataoka, K. *J. Control. Release* **2001**, *77*, 27.
(32) Seymour, L. W.; Duncan, R.; Strohalm, J.; Kopecek, J. *J. Biomed. Mater. Res.* **1987**, *21*, 1341.
(33) Rekatas, C. J.; Mai, S.-M.; Crothers, M.; Quinn, M.; Collett, J. H.; Attwood, D.; Heatley, F.; Martini, L.; Booth, C. *Phys. Chem. Chem. Phys.* **2001**, *3*, 4769.
(34) Booth, C; Attwood, D. *Macromol. Rapid Commun.* **2000**, *21*, 501.
(35) Lavasanifar, A.; Samuel, J.; Kwon, G. S. *Colloid Surf. B-Biointerfaces* **2001**, *22*, 115.
(36) Müller, A.; Burchard, W. *Colloid Polym. Sci.* **1995**, *273*, 866.
(37) Crothers, M.; Attwood, D.; Collett, J. H.; Yang, Z.; Booth, C.; Taboada, P.; Mosquera, V.; Ricardo, N. M. P. S.; Martini, L. G. A. *Langmuir* **2002**, 18, 8685.
(38) Rangel-Yagui, C. O.; Pessoa-Jr, A.; Tavares, L. C. *J. PHARM. PHARM. SCI.* **2005**, *8*, 147.
(39) Nagarajan, R. *Colloid Surf. B-Biointerfaces* **1999**, *16*, 55.
(40) Zhange, X.; Jackson, J. K.; Burt, H. M. *Int. J. Pharm.* **1996**, *132*, 195.
(41) Fournier, E.; Dufresne, M. H.; Smith, D. C.; Ranger, M.; Leroux, J. C. *Pharm. Res.* **2004**, *21*, 962.
(42) Liu, J.; Xiao, Y.; Allen, C. *J. Pharm. Sci.* **2004**, *93*, 132.

BM070226V